J Shanghai Univ (Engl Ed), 2009, 13(1): 29–36
Digital Object Identifier(DOI): 10.1007/s 11741-009-0107-2

Maximum power point tracking of a photovoltaic energy system using neural fuzzy techniques

LI Chun-hua (李春华)[1], ZHU Xin-jian (朱新坚)[1], SUI Sheng (隋 升)[1], HU Wan-qi (胡万起)[2]
1. Fuel Cell Research Institute, Shanghai Jiaotong University, Shanghai 200240, P. R. China
2. Institute of Process Engineering, Chinese Academy of Sciences, Beijing 100080, P. R. China

Abstract In order to improve the output efficiency of a photovoltaic (PV) energy system, the real-time maximum power point (MPP) of the PV array should be tracked closely. The non-linear and time-variant characteristics of the photovoltaic array and the non-linear and non-minimum phase characteristics of a boost converter make it difficult to track the MPP as in traditional control strategies. A neural fuzzy controller (NFC) in conjunction with the reasoning capability of fuzzy logical systems and the learning capability of neural networks is proposed to track the MPP in this paper. A gradient estimator based on a radial basis function neural network is developed to provide the reference information to the NFC. With a derived learning algorithm, the parameters of the NFC are updated adaptively. Experimental results show that, compared with the fuzzy logic control algorithm, the proposed control algorithm provides much better tracking performance.

Keywords photovoltaic array, boost converter, maximum power point tracking (MPPT), neural fuzzy controller (NFC), radial basis function neural networks (RBFNN)

Introduction

Photovoltaic (PV) energy systems that convert the solar energy directly to electrical energy are becoming more popular due to the scarcity and adverse environmental impacts of conventional fossil fuels. In order to improve the output efficiency of PV arrays, it is crucial to operate PV energy systems near maximum power point (MPP). Generally, a DC-DC converter linking the PV array and the load is used to carry out the maximum power point tracking (MPPT) of the PV system by tuning its duty ratio[1]. The boost converter is preferred due to its advantages over the buck converter[2]. However, the MPP of the PV array varies with the solar insolation and environmental temperature as shown in Fig.1. Furthermore, the PV array exhibits extremely non-linear voltage-current characteristics. Its output power depends on the terminal load of the PV system. The non-linear and non-minimum phase characteristics of the boost converter[3] complicate the MPPT further. To overcome these difficulties, some control strategies have been proposed such as constant voltage[4], perturbing and observing[5], incremental conductance[6], sliding mode[7], fuzzy logic control[8−9] and neural network[10−11]. However, there still remains a problem of quickly and accurately determining the locus of the MPP when parameter variations and external load disturbances occur.

Both fuzzy logic controller (FLC) and neural network controller (NNC) have been successfully used in many applications. The fuzzy IF-THEN rules extracted from the expert knowledge are used to express proper control strategy. Therefore, a precise mathematical model of the plant is not required for the FLC. It is difficult, however, to design the FLC systematically. Furthermore, the static FLC behavior relies significantly on expertise knowledge and has no mechanisms for adapting to the real-time plant change. On the other hand, a neural network possesses the strong capability of learning from the process apart from parallelism and fault tolerance. A learning algorithm is usually used to update the parameters of the network architecture. But it needs a tremendous amount of training data and takes a long time to carry out the preliminary offline learning. It is often difficult to decide how complex a structure is actually necessary for the desired control. In addition, the inside operating of the networks are invisible to the designer. A neural fuzzy controller (NFC)[12−14], the combination of an FLC and an NNC, is one of the best controllers to solve these problems. The NNC pro-

Received Feb.26, 2008; Revised Jul.11, 2008
Project supported by the National Natural Science Foundation of China (Grant No.20576071)
Corresponding author LI Chun-hua, PhD Candidate, E-mail: viven_lch@sjtu.edu.cn

vides the connectionist structure and learning ability to the FLC; the FLC provides a structural framework with fuzzy IF-THEN rule reasoning to the NNC.

In this study, a novel control algorithm is developed for the MPPT of the PV energy system. A four-layer NFC is designed to track the MPP. The information extracted from the fuzzy control experiences is used to initialize the parameters of the NFC. An on-line learning algorithm based on the back-propagation method is derived to update the parameters of the NFC adaptively. A radial basis function neural network (RBFNN) is used as the gradient estimator in order to provide the reference information to the NFC. Compared with the traditional fuzzy logic controller, some experiments are performed to validate the efficiency of the proposed control strategy. Finally, conclusion is presented.

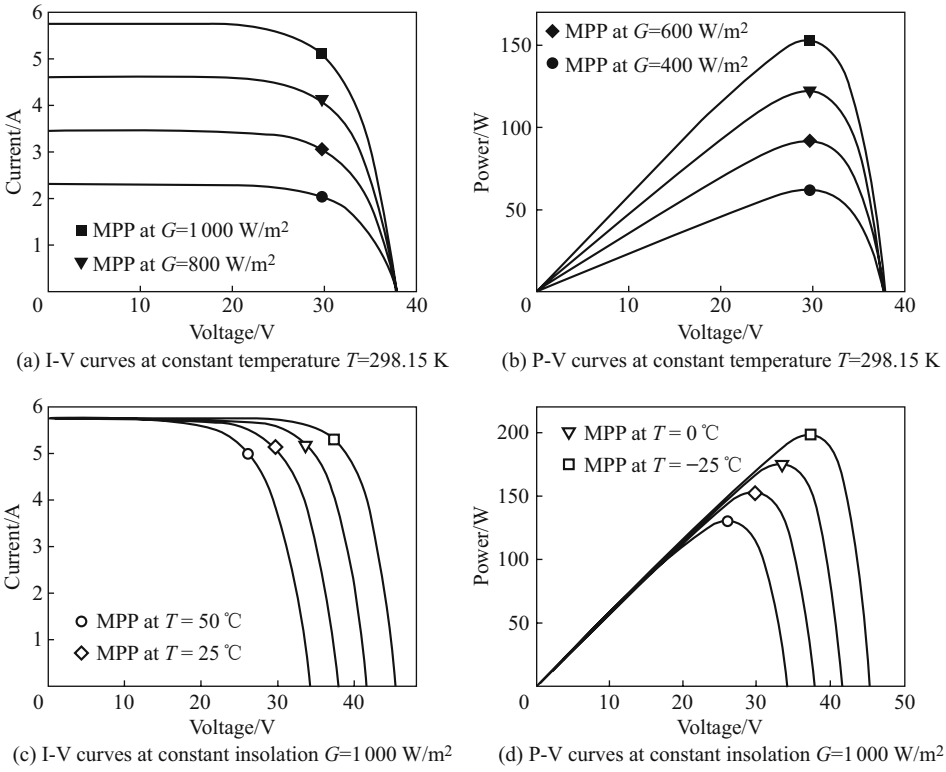

(a) I-V curves at constant temperature T=298.15 K (b) P-V curves at constant temperature T=298.15 K

(c) I-V curves at constant insolation G=1 000 W/m^2 (d) P-V curves at constant insolation G=1 000 W/m^2

Fig.1 I-V and P-V characteristic curves of the PV array

1 Photovoltaic energy system

A schematic overview of the PV energy system is shown in Fig.2. This system consists of a PV array and a boost converter. The dynamic model of the system can be expressed as [15]:

$$\begin{cases} \dfrac{\mathrm{d}v_{\mathrm{PV}}}{\mathrm{d}t} = \dfrac{1}{C_1}(i_{\mathrm{PV}} - i_{L_C}), \\ \dfrac{\mathrm{d}i_{L_C}}{\mathrm{d}t} = \dfrac{1}{L_C}(v_{\mathrm{PV}} - vC_2(1-D)), \\ \dfrac{\mathrm{d}v_{C_2}}{\mathrm{d}t} = \dfrac{1}{C_2}\Big(i_{L_C}(1-D) - \dfrac{v_{C_2}}{R_L}\Big). \end{cases} \tag{1}$$

1.1 Photovoltaic array

As a function of voltage, the current of the PV array is defined as [16]:

$$i_{\mathrm{PV}} = n_{\mathrm{p}} I_{\mathrm{ph}} - n_{\mathrm{p}} I_D \Big[\exp\Big(\frac{v_{\mathrm{PV}} + R_{\mathrm{s}} i_{\mathrm{PV}}}{n_{\mathrm{s}} v_{\mathrm{t}}}\Big) - 1\Big], \tag{2}$$

where n_{s} is the number of PV cells connected in series; n_{p} is the number of the cells in parallel; v_{t} is the thermal voltage.

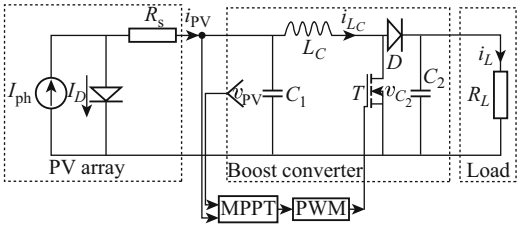

Fig.2 Photovoltaic energy system

The characteristics of the PV array are non-linear and time-variant in nature. The output power of solar cell increases with an increase in solar radiation and decreases with an increase in temperature as shown in Fig.1. There is a unique MPP on each P-V curve. The

MPP must be tracked using a maximum power point tracker in order to extract maximum power from the PV array.

1.2 Boost converter

Boost converter as shown in Fig.2 is used to track the MPP by tuning its duty ratio $D(0 \leqslant D \leqslant 1)$. According to the duty ratio given by the MPPT, a pulse width modulation (PWM) method is used to generate pulse and drive the MOSFET T. The boost converter is characterized by the non-linearity and non-minimum phase. The equivalent input resistance of the boost converter can be calculated by [17]

$$R_{\rm eq} = R_i(1-D)^2. \tag{3}$$

According to the power transfer theory, the power delivered to the load is maximized when the equivalent resistance $R_{\rm eq}$ equals to the output resistance of the PV array[18].

2 Proposed neural fuzzy controller

The proposed intelligent control system is schematically shown in Fig.3. An adaptive neural fuzzy controller (NFC) is adopted as the maximum power point tracker. The condition of a maximum power point can be described as

$$\frac{\partial P_{\rm pv}}{\partial v_{\rm pv}} = \frac{\partial v_{\rm pv} i_{\rm pv}}{\partial v_{\rm pv}} = v_{\rm pv}\frac{\partial i_{\rm pv}}{\partial v_{\rm pv}} + i_{\rm pv} = 0. \tag{4}$$

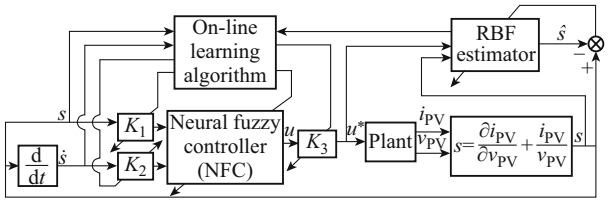

Fig.3 Adaptive neural fuzzy control system

Hence, input error term of the NFC for the MPP can be calculated as

$$\begin{aligned} s &= \frac{\partial i_{\rm pv}}{\partial v_{\rm pv}} + \frac{i_{\rm pv}}{v_{\rm pv}} \\ &\approx \frac{i_{\rm pv}(N) - i_{\rm pv}(N-1)}{v_{\rm pv}(N) - v_{\rm pv}(N-1)} + \frac{i_{\rm pv}(N)}{v_{\rm pv}(N)}, \end{aligned} \tag{5}$$

where N is the number of iterations. The RBFNN-based estimator is designed to identify the input-output dynamic behavior of the controlled plant so as to provide a reference signal for the NFC parameter tuning.

2.1 Structure of the NFC

Figure 4 depicts the NFC structure, which is a four-layer feedforward connectionist network to realize a simplified fuzzy inference system[12]. Let each input have n membership functions, then the input-output relations between layers are stated precisely as follows:

(i) Layer 1: input layer

The input units in this layer are the tracking error $x_1 = k_1 s$ and the change of the error $x_2 = k_2 \dot{s}$. The input layer is defined as

$$\begin{cases} I_i^{(1)} = x_i, \quad i = 1, 2, \\ O_{ij}^{(1)} = I_i^{(1)}, \quad j = 1, 2, \cdots, n. \end{cases} \tag{6}$$

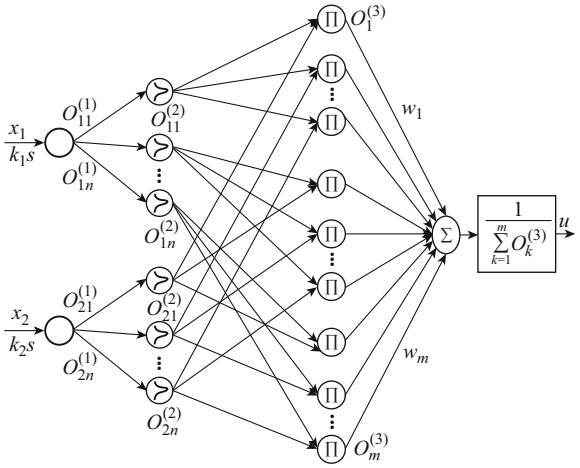

Fig.4 Structure of the four-layer NFC

(ii) Layer 2: linguistic term layer

In this layer, each node uses a Gaussian function as a membership function. Thus, the input-output relationship of this layer is defined as

$$\begin{cases} I_{ij}^{(2)} = -\dfrac{(O_{ij}^{(1)} - a_{ij})^2}{b_{ij}^2}, \\ O_{ij}^{(2)} = \exp(I_{ij}^{(2)}), \end{cases} \tag{7}$$

where a_{ij} and b_{ij} are, respectively, the center and the width parameters of the Gaussian function.

(iii) Layer 3: rule layer

Each node in this layer is denoted by Π. The rule node is represented as

$$\begin{cases} I_{(j-1)n+l}^{(3)} = O_{1j}^{(2)} O_{2l}^{(2)}, \quad l = 1, 2, \cdots, n, \\ O_k^{(3)} = I_k^{(3)}, \quad k = 1, 2, \cdots, m(= n^2). \end{cases} \tag{8}$$

(v) Layer 4: output layer

This layer performs the centroid defuzzification to obtain the inference output, that is

$$\begin{cases} I^{(4)} = \sum_{k=1}^{m} O_k^{(3)} w_k, \\ O^{(4)} = u = \dfrac{I^{(4)}}{\sum_{k=1}^{m} O_k^{(3)}}. \end{cases} \tag{9}$$

The control input of the plant is defined as

$$u^* = k_3 u. \tag{10}$$

2.2 On-line learning algorithm

Once an NFC has been constructed, the learning aims at determining appropriate values for the quantization factors (k_1, k_2), the scale factor (k_3), the parameters of the Gaussian membership functions (a_{ij}, b_{ij}), and the linking weights (w_q). Instead of using random numbers in pure neural networks, we suggest in this study to initialize these parameters using the expert knowledge from the traditional fuzzy control. These initial settings can generally give more meaningful and stable starting than random initialization. After the initialization process, a gradient-descent-based back-propagation algorithm is employed to adjust the controller parameters.

The error function is defined as

$$E = \frac{1}{2} k_1 s^2. \tag{11}$$

The scale factor and the linking weights are updated by

$$\frac{\partial E}{\partial k_3} = \frac{\partial E}{\partial s}\frac{\partial s}{\partial u^*}\frac{\partial u^*}{\partial k_3} = k_1 s \frac{\partial s}{\partial u^*} u, \tag{12}$$

$$\begin{aligned} \frac{\partial E}{\partial w_q} &= \frac{\partial E}{\partial s}\frac{\partial s}{\partial u^*}\frac{\partial u^*}{\partial u}\frac{\partial u}{\partial w_q} \\ &= k_1 s \frac{\partial s}{\partial u^*} k_3 \frac{O_k^{(3)}}{\sum_{p=1}^{m} O_p^{(3)}}. \end{aligned} \tag{13}$$

The gradients $\frac{\partial E}{\partial a_{1j}}$ and $\frac{\partial E}{\partial k_1}$ can be derived respectively by

$$\begin{aligned} \frac{\partial E}{\partial a_{1j}} &= \frac{\partial E}{\partial s}\frac{\partial s}{\partial u^*}\frac{\partial u^*}{\partial u}\sum_{l=1}^{n}\frac{\partial u}{\partial O_{(j-1)n+l}^{(3)}} \\ &\quad \cdot \frac{\partial O_{(j-1)n+l}^{(3)}}{\partial O_{1j}^{(2)}}\frac{\partial O_{1j}^{(2)}}{\partial I_{1j}^{(2)}}\frac{\partial I_{1j}^{(2)}}{\partial a_{1j}} \\ &= k_1 s \frac{\partial s}{\partial u} k_3 \frac{2(O_{1j}^{(1)} - a_{1j}) O_{1j}^{(2)}}{b_{1j}^2 \Big(\sum_{p=1}^{m} O_p^{(3)}\Big)^2} \sum_{l=1}^{n} O_{2l}^{(2)} \\ &\quad \cdot \Big(w_{(j-1)n+l} \sum_{p=1}^{m} O_p^{(3)} - \sum_{p=1}^{m} O_p^{(3)} w_p\Big), \\ &\quad j = 1, 2, \cdots, n, \end{aligned} \tag{14}$$

$$\frac{\partial E}{\partial k_1} = \sum_{j=1}^{n}\Big(-\frac{\partial E}{\partial a_{1j}}\Big) s. \tag{15}$$

In a similar way, the gradients $\frac{\partial E}{\partial a_{2j}}$ and $\frac{\partial E}{\partial k_2}$ can be derived respectively by

$$\begin{aligned} \frac{\partial E}{\partial a_{2j}} &= k_1 s \frac{\partial s}{\partial u^*} k_3 \frac{2(O_{2j}^{(1)} - a_{2j}) O_{2j}^{(2)}}{b_{2j}^2 \Big(\sum_{p=1}^{m} O_p^{(3)}\Big)^2} \sum_{l=1}^{n} O_{1l}^{(2)} \\ &\quad \cdot \Big(w_{(l-1)n+j} \sum_{p=1}^{m} O_p^{(3)} - \sum_{p=1}^{m} O_p^{(3)} w_p\Big), \\ &\quad j = 1, 2, \cdots, n, \end{aligned} \tag{16}$$

$$\frac{\partial E}{\partial k_2} = \sum_{j=1}^{n}\Big(-\frac{\partial E}{\partial a_{2j}}\Big)\dot{s}. \tag{17}$$

The gradients $\frac{\partial E}{\partial b_{1j}}$ and $\frac{\partial E}{\partial b_{2j}}$ can be obtained by

$$\begin{aligned} \frac{\partial E}{\partial b_{1j}} &= k_1 s \frac{\partial s}{\partial u^*} k_3 \frac{2(O_{1j}^{(1)} - a_{1j})^2 O_{1j}^{(2)}}{b_{1j}^3 \Big(\sum_{p=1}^{m} O_p^{(3)}\Big)^2} \sum_{l=1}^{n} O_{2l}^{(2)} \\ &\quad \cdot \Big(w_{(j-1)n+l} \sum_{p=1}^{m} O_p^{(3)} - \sum_{p=1}^{m} O_p^{(3)} w_p\Big), \\ &\quad j = 1, 2, \cdots, n, \end{aligned} \tag{18}$$

$$\begin{aligned} \frac{\partial E}{\partial b_{2j}} &= k_1 s \frac{\partial s}{\partial u^*} k_3 \frac{2(O_{2j}^{(1)} - a_{2j})^2 O_{2j}^{(2)}}{b_{2j}^3 \Big(\sum_{p=1}^{m} O_p^{(3)}\Big)^2} \sum_{l=1}^{n} O_{1l}^{(2)} \\ &\quad \cdot \Big(w_{(l-1)n+j} \sum_{p=1}^{m} O_p^{(3)} - \sum_{p=1}^{m} O_p^{(3)} w_p\Big), \\ &\quad j = 1, 2, \cdots, n. \end{aligned} \tag{19}$$

Then, the NFC parameters can be updated by [12]

$$\begin{cases} w_q(N+1) = w_q(N) - \eta \dfrac{\partial E}{\partial w_q} + \beta \Delta w_q(N), \\ a_{ij}(N+1) = a_{ij}(N) - \eta \dfrac{\partial E}{\partial a_{ij}} + \beta \Delta a_{ij}(N), \\ b_{ij}(N+1) = b_{ij}(N) - \eta \dfrac{\partial E}{\partial b_{ij}} + \beta \Delta b_{ij}(N), \\ k_c(N+1) = k_c(N) - \eta \dfrac{\partial E}{\partial k_c} + \beta \Delta k_c(N), \end{cases} \tag{20}$$

$$\Delta\chi = \chi(N) - \chi(N-1), \quad q = 1, 2, \cdots, m, \quad c = 1, 2, 3.$$

The only unknown in the proposed learning algorithm is $\frac{\partial s}{\partial u^*}$ the gradient of the system output with respect to the control input. Many schemes in literature can be utilized to evaluate this gradient[12−14]. In this work, we attempt to develop an online gradient estimator based on RBFNN.

2.3 RBFNN-based gradient estimator

A three-layer feedforward RBFNN[19] as shown in Fig.5 is adopted to estimate the gradient $\frac{\partial s}{\partial u^*}$. The input of the network is the control input ($\widetilde{x}_1 = u^*$) and the output of the controlled plant ($\widetilde{x}_2 = s$). The output of the RBFNN is the estimated value $\hat{s}$ of the tracking error s. The signal propagation and the activation function in each layer are introduced as

(i) Input layer

$$\begin{cases} \text{net}_r^{(1)} = \widetilde{x}_r, \quad r = 1, 2, \\ y_r^{(1)} = \text{net}_r^{(1)}, \quad r = 1, 2. \end{cases} \tag{21}$$

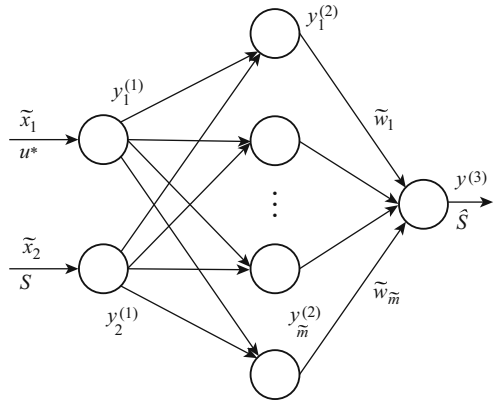

Fig.5 Structure of three-layer RBFNN estimator

(ii) Hidden layer

$$\begin{cases} \text{net}_v^{(2)} = -\dfrac{(y_1^{(1)} - \phi_{1v})^2 + (y_2^{(1)} - \phi_{2v})^2}{2\sigma_v^2}, \\ y_v^{(2)} = \exp(\text{net}_v^{(2)}), \quad v = 1, 2, \cdots, \widetilde{m}. \end{cases} \tag{22}$$

(iii) Output layer

$$\begin{cases} \text{net}^{(3)} = \displaystyle\sum_{v=1}^{\widetilde{m}} \widetilde{w}_v y_v^{(2)}, \\ y^{(3)} = \text{net}^{(3)}. \end{cases} \tag{23}$$

The error function of the RBFNN is defined as

$$e = \frac{1}{2}(s - \hat{s})^2. \tag{24}$$

The parameters $(\phi_{rv}, \sigma_v, \widetilde{w}_v)$ can be updated by

$$\begin{cases} \widetilde{w}_v(N+1) = \widetilde{w}_v(N) - \widetilde{\eta}\dfrac{\partial e}{\partial \widetilde{w}_v} + \widetilde{\beta}\Delta\widetilde{w}_v(N), \\ \phi_{rv}(N+1) = \phi_{rv}(N) - \widetilde{\eta}\dfrac{\partial e}{\partial \phi_{rv}} + \widetilde{\beta}\Delta\phi_{rv}(N), \\ \sigma_v(N+1) = \sigma_v(N) - \widetilde{\eta}\dfrac{\partial e}{\partial \sigma_v} + \widetilde{\beta}\Delta\sigma_v(N). \end{cases} \tag{25}$$

Mean square error (MSE) is employed here to evaluate identification results:

$$\text{MSE} = \frac{1}{N}\sum_{t=1}^{N}(s(t) - \hat{s}(t))^2. \tag{26}$$

From the input-output relationship between $\hat{s}$ and u^* of the RBFNN, we can get the required gradient information for the NFC as

$$\begin{aligned} \frac{\partial s}{\partial u^*} \approx \frac{\partial \hat{s}}{\partial u^*} &= \sum_{v=1}^{\widetilde{m}} \frac{\partial \hat{s}}{\partial y^{(3)}} \frac{\partial y^{(3)}}{\partial y_v^{(2)}} \frac{\partial y_v^{(2)}}{\text{net}_v^{(2)}} \frac{\text{net}_v^{(2)}}{\partial u^*} \\ &= \sum_{v=1}^{\widetilde{m}} \widetilde{w}_v y_v^{(2)} \frac{(\phi_{1v} - y_1^{(1)})}{\sigma^2}. \end{aligned} \tag{27}$$

3 Results and discussion

In this section, we shall implement the proposed NFC to track the MPP of the PV array. The parameters in the NFC are initialized as follows:

$$\begin{aligned} &k_1 = 1, \quad k_2 = 0.50, \quad k_3 = 1, \\ &\eta = 0.30, \quad \beta = 0.02, \quad n = 7, \\ &[a_{i1}(0), a_{i2}(0), \cdots, a_{in}(0)] \\ &\quad = [-1, -2/3, -1/3, 0, 1/3, 2/3, 1], \quad b_{ij}(0) = 0.25. \end{aligned}$$

The initial linking weights $\boldsymbol{w}$ are listed in Table 1. The parameters of the RBFNN are initialized as

$$\begin{aligned} &\widetilde{\eta} = 0.35, \quad \widetilde{\beta} = 0.05, \\ &\widetilde{w}_v = 0, \quad \phi_{rv} = 0.10, \quad \sigma_v = 3, \\ &r = 1.20, \quad v = 1, \cdots, \widetilde{m}, \quad \widetilde{m} = 4. \end{aligned}$$

In order to show the effectiveness of the proposed control algorithm, a traditional FLC is also used to track the MPP[8]. The atmospheric conditions (insolation and temperature) and external load disturbance are shown in Fig.6. The quantization factors (k_1, k_2) and scale factor (k_3) are adaptive to condition variations as shown in Fig.7. The comparison between the experimental error s and the error $\hat{s}$ acquired by the RBFNN is shown in Fig.8. The MSE of the error s is 0.005 4. Figures 9 and 10 depict the voltage and current of the PV array regulated by MPP tracker, respectively. The traditional

Table 1 Initial linking weights of the NFC

x_2	x_1						
	NB	NM	NS	ZO	PS	PM	PB
NB	$1.00(w_1)$	$1.00(w_8)$	0.66	0.66	0.33	0.33	0.00
NM	$1.00(w_2)$	0.66	0.66	0.33	0.33	0.00	−0.33
NS	0.66	0.66	0.33	0.33	0.00	−0.33	−0.33
ZO	0.66	0.33	0.33	0.00	−0.33	−0.33	−0.66
PS	0.33	0.33	0.00	−0.33	−0.33	−0.66	−0.66
PM	0.33	0.00	−0.33	−0.33	−0.66	−0.66	$-1.00(w_{48})$
PB	0.00	−0.33	−0.33	−0.66	−0.66	$-1.00(w_{42})$	$-1.00(w_{49})$

FLC needs 8 ms to reach sable state and its overshoot is big. Comparatively, the proposed algorithm is better than the traditional FLC, and it only needs no more than 2 ms with hardly any overshoot to reach steady state.

The error s of the maximum power point tracking is shown in Fig.11. Although both of the FLC and the proposed NFC can acquire the MPP under the variant conditions, the accuracy and stability achieved by the proposed NFC is better than that of the FLC.

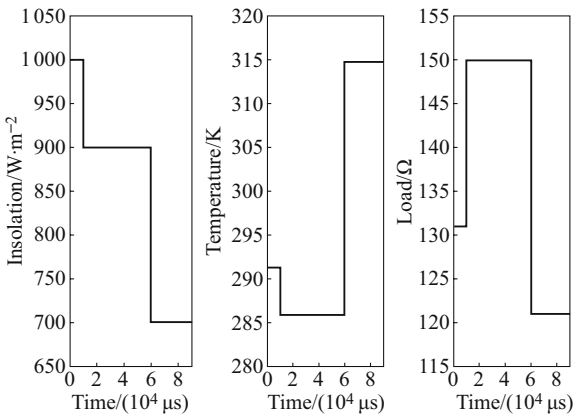

Fig.6 Insolation, temperature and load

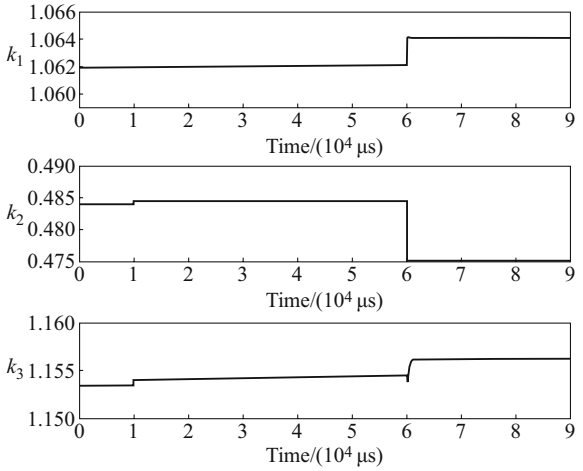

Fig.7 Quantization factors (k_1, k_2) and scale factor (k_3)

4 Conclusion

In this paper, an intelligent control strategy is proposed for the MPPT of a PV energy system. A four-layer NFC is adopted as the process feedback controller.

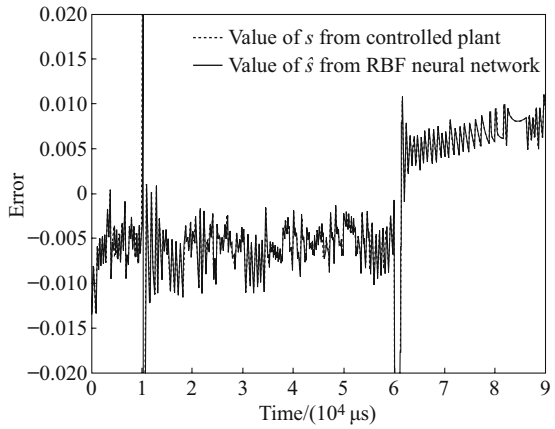

Fig.8 Comparison between the experimental error s and the error $\hat{s}$ acquired by the RBFNN

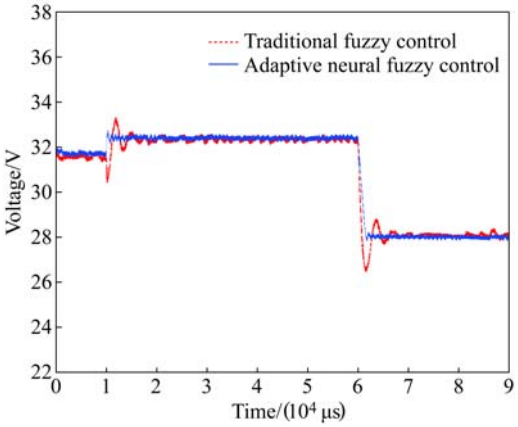

Fig.9 Regulated voltage (v_{PV}) of photovoltaic energy system

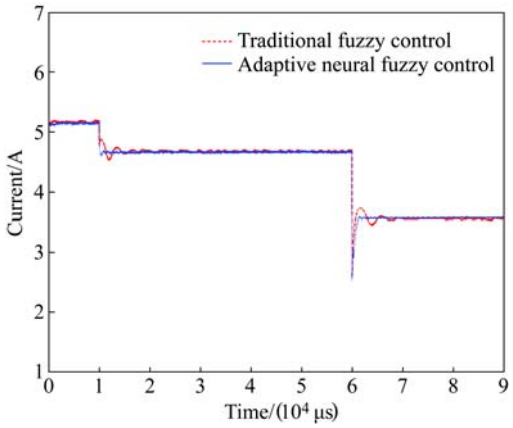

Fig.10 Regulated current (i_{PV}) of photovoltaic energy system

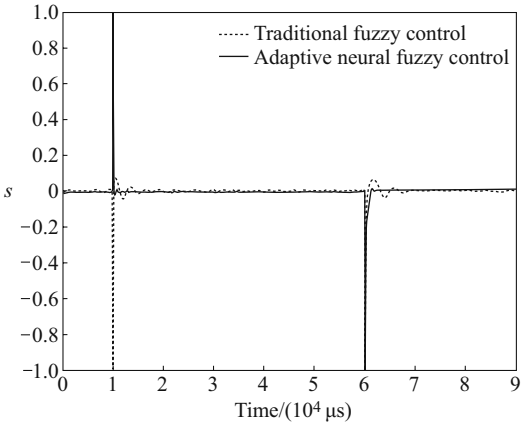

Fig.11 Error (s) of MPPT for the photovoltaic energy system

The NFC is initialized using the expert knowledge from the traditional fuzzy control, which reduces the burden of the lengthy pre-learning. With a derived learning algorithm, the parameters in the NFC are updated adaptively by observing the tracking error s. A radial basis function neural network (RBFNN) is designed to provide the NFC with the gradient information, which reduces the complexity of the internal system. The experimental results have shown that the NFC can track the MPP smoothly and quickly, exhibits good robustness to the parameter variants and external load disturbances, and performs much better compared with the traditional FLC.

References

[1] Xiao W D, Dunford W G, Palmer, P R, *et al.* Regulation of photovoltaic voltage [J]. IEEE Transactions on Industrial Electronics, 2007, 54(3): 1365–1374.

[2] Xiao W D, Ozog N, Dunford W G. Topology study of photovoltaic interface for maximum power point tracking [J]. IEEE Transactions on Industrial Electronics, 2007, 54(3): 1696–1704.

[3] Shtessela Y B, Zinober A S I, Shkolnikov Il A. Sliding mode control of boost and buck-boost power converters using method of stable system centre [J]. Automatica, 2003, 39(6): 1061–1067.

[4] Swiegers W, Enslin J H R. An integrated maximum power point tracker for photovoltaic panels [C]// Proceedings of IEEE International Symposium on Industrial Electronics, Pretoria, South Africa. Piscataway, NJ, USA: IEEE Press, 1998: 40–44.

[5] Santos J L, Antunes F, Chehab A, *et al.* A maximum power point tracker for PV systems using a high performance boost converter [J]. Solar Energy, 2006, 80(7): 772–778.

[6] Brambilla A. New approach to photovoltaic arrays maximum power point tracking [C]// Proceeding of the 30th IEEE Power Electronics Specialists Conference, South Carolina, USA. Piscataway, NJ, USA: IEEE Press, 1998: 632–637.

[7] Valenciaga F, Puleston P F, Battaiotto P E. Power control of a photovoltaic array in a hybrid electric generation system using sliding mode techniques [J]. IEE Proceedings of Control Theory and Application, 2001, 148(6): 448–455.

[8] Patcharaprakiti N, Premrudeepreechacharn S, Sriuthaisiriwong Y. Maximum power point tracking using adaptive fuzzy logic control for grid-connected photovoltaic system [J]. Renewable Energy, 2005, 30(1): 1771–1788.

[9] Altasa I H, Sharaf A M. A novel maximum power fuzzy logic controller for photovoltaic solar energy systems [J]. Renewable Energy, 2008, 33(3): 388–399.

[10] Hiyama T, Kouzuma S, Imakubo T, *et al.* Evaluation of neural network based real time maximum power tracking controller for PV system [J]. IEEE Transactions on Energy Conversion, 1995, 10(3): 543–548.

[11] Torres A M, Antunes F L M. An artificial neural network-based real time maximum power tracking controller for connecting a PV system to the grid [C]// The 24th Annual Conference of the IEEE Industrial Electronics Society, Aachen, Germany. Piscataway, NJ, USA: IEEE Press, 1998: 554–558.

[12] Chen C T, Peng S T. Intelligent process control using neural fuzzy techniques [J]. Journal of Process Control, 1999, 9(6): 493–503.

[13] Qi Z D, Zhu X J, Cao G Y. Nonlinear modeling of molten carbonate fuel cell stack and EGA-based fuzzy control [J]. Journal of Shanghai University (English Edition), 2006, 10(2): 144–150.

[14] Lin F J, Shen P H. Adaptive fuzzy-neural-network control for a DSP-based permanent magnet linear synchronous motor servo drive [J]. IEEE Transactions on Fuzzy Systems, 2006, 14(4): 481–495.

[15] Das D, Esmaili R, Xu L Y, *et al.* An optimal design of a grid connected hybrid wind/photovoltaic/fuel cell system for distributed energy production [C]// The 32nd Annual Conference of the IEEE Industrial Electronics Society, Paris, France. Piscataway, NJ, USA: IEEE Press, 2005: 2499–2504.

[16] Xiao W D, Dunford W G, Capel A. A novel modeling method for photovoltaic cells [C]// IEEE Power Electronics Specialists Conference, Aachen, Germany. Piscataway, NJ, USA: IEEE Press, 2004: 1950–1956.

[17] Kazimierczuk M K, Starman L A. Dynamic performance of PWM DC-DC boost converter with input voltage feedforward control [J]. IEEE Transactions on Fundamental Theory and Applications, 1999, 46(12): 1473–1481.

[18] Mukerjee A K, Dasgupta N. DC power supply used as photovoltaic simulator for testing MPPT algorithms [J]. Renewable Energy, 2007, 32(4): 587–592.

[19] Huang S J, Huang K S, Chiou K C. Development and application of a novel radial basis function sliding mode controller [J]. Mechatronics, 2003, 13(4): 313–329.

(Editor HONG Ou)